EUROSUN2026

ADVANCED LOW-EMISSIVITY AND ROBUST MULTILAYER SELECTIVE COATINGS FOR HIGH-VACUUM FLAT PLATE SOLAR COLLECTORS

Benedetta Francine Catalano[1,4], Antonio Caldarelli[2], Carmine D'Alessandro[5], Eliana Gaudino[1,4], Alessandro Vitaliano Anacreonte[1,3], Fabio Capolupo[1,3], Annalisa Di Napoli[1,3], Mara Pesapane[1,3], Marilena Musto[1,3], Roberto Russo[1], Emiliano Di Gennaro[1,4]

[1] Institute of Applied Sciences and Intelligent Systems, National Research Council of Italy, Naples, Italy
[2] Institute for Superconductors, Innovative Materials and Devices,National Research Council of Italy, Naples, Italy
[3] Industrial Energy Department, University of Naples "Federico II", Naples, Italy
[4] Physics Department, University of Naples "Federico II", Naples, Italy
[5] TVP Solar SA, Satigny, Switzerland

benedetta.catalano@na.isasi.cnr.it; antonio.caldarelli@na.isasi.cnr.it; dalessandro@tvpsolar.com; eliana.gaudino@na.isasi.cnr.it; alessandro.anacreonte@na.isasi.cnr.it; fabio.capolupo@na.isasi.cnr.it; annalisa.dinapoli@na.isasi.cnr.it; mara.pesapane@na.isasi.cnr.it; marilena.musto@unina.it; roberto.russo@na.isasi.cnr.it; emiliano.digennaro@unina.it.

Summary

The decarbonisation of industrial process heat requires efficient solar thermal technologies capable of operating at medium temperatures (100-300 °C). High-Vacuum Flat Plate Collectors (HVFPCs) represent a promising solution. This work proposes a combined strategy based on multilayer coating optimisation and low-emissivity thin films. Cr_2O_3/Cr multilayers are optimised via a genetic algorithm, ensuring robustness against thickness variations, while Ag coatings reduce radiative losses. The framework is further extended to account for the solar spectrum effectively transmitted through the glass envelope, enabling a more realistic optimisation criterion with only a limited impact on the overall collector performance. In addition, the genetic algorithm is also allowed to explore alternative multilayer architectures beyond the reference $\mathrm{Cr_2O_3/Cr}$ structure. The results show high solar absorptance, up to 0.97, and thermal emittance values as low as approximately 0.025 over the investigated temperature range, while the introduction of low-emissivity backside configuration leads to relative efficiency improvements of approximately 10% at 300 °C. Moreover, the extended material optimisation provides further efficiency improvements of approximately 6–8% at 300 °C.

Keywords: selective solar absorber, low-emissivity coating, HVFPC, multilayer coatings, genetic algorithm, conversion efficiency.

Field of application for the findings: Solar thermal collectors, industrial heat, renewable energy systems.

Addressed audience: Researchers, engineers and industry professionals in solar thermal energy.

1. Introduction

The transition to renewable energy sources is a key challenge in reducing greenhouse gas emissions, particularly in the industrial sector, which accounts for a significant fraction of global energy consumption. Half of the global industrial process heat demand is in the low and medium-temperature range (<400 °C), with about 35% below 150 °C and 15% between 150 and 400 °C (IEA, 2022). Currently, this demand is fulfilled by fossil fuels (IEA, 2018), but solar thermal technologies offer a viable alternative. However, conventional flat plate collectors are typically limited to temperatures below 100 °C.

In contrast, High Vacuum Flat Plate Collectors (HVFPCs) enable operation at higher temperatures by suppressing convective losses through vacuum insulation (Moss et al., 2018; Gao et al., 2020). In these systems, radiative losses become dominant, which makes the optimisation of Selective Solar Absorbers (SSAs) crucial (De Maio et al., 2022). Theoretically, the ideal SSA spectral emissivity is represented by a step-function value of 1 in the solar range and 0 in the infrared range, where the cut-off wavelength ($\lambda_{cut-off}$) is the point where spectral emissivity shifts, marking the intersection of the solar radiation with the blackbody radiation curves (Burlafinger et al., 2015). This is demonstrated to maximise the thermal conversion performance of the absorber. Since the blackbody radiation shifts with temperature, the overlap with the solar spectrum happens at lower wavelengths as the operating temperature increases (Ning et al., 2020).

Moving to practical devices, the optimisation process of a real SSA is largely affected by some important non-ideal characteristics such as the non-null thermal emittance, the non-unitary solar absorption, and the slope width of the emissivity curve in the transition from high to low spectral emissivity, which occurs over a non-zero wavelength interval, covering part of the solar spectral irradiance range. These characteristics worsen thermal radiation losses, especially at elevated temperatures, where they increase with the fourth power of temperature (Caldarelli et al., 2023). Addressing these practical limitations requires design strategies capable of tailoring the spectral response of the device. On the front-side, recent studies have focused on multilayer coatings based on metal–dielectric stacks, which allow precise tuning of optical properties through interference effects (Zhou et al., 2024). At the same time, reducing the absorber substrate's emissivity by means of a low-emissivity coating (LEC) provides an additional means of limiting radiative heat losses.

For a solar thermal collector, however, the coating performance cannot be assessed only from its optical properties. Thermal efficiency is determined by the balance between the useful solar power absorbed by the system and the thermal losses dissipated towards the environment. In conventional collectors, both convective and radiative losses contribute to the thermal loss budget, whereas in High-Vacuum Flat Plate Collectors (HVFPCs), vacuum insulation largely suppresses convective heat transfer. Consequently, radiative losses become the dominant limitation at medium-to-high operating temperatures, making the balance between solar absorptance and temperature-dependent thermal emittance extremely critical. This also implies that the relative importance of the spectral regions contributing to solar absorption and thermal emission changes with the operating temperature. Therefore, the optimisation of a selective solar absorber should ideally be formulated in terms of the actual thermal efficiency of the collector under the prescribed operating conditions, rather than through independently optimised optical parameters.

Standard coating optimisation approaches often assign predefined weights to solar absorptance and thermal emittance, while deviations related to manufacturing processes are generally treated separately from the optical optimisation. To overcome these limitations, the present work proposes a comprehensive optimisation framework, in which a genetic algorithm directly maximises the overall thermal efficiency while accounting for prescribed layer-thickness deviations.

The framework further considers the spectral transmittance of the glass envelope by weighting the reference AM1.5 solar spectrum with its wavelength-dependent transmittance, thus providing a more realistic representation of the solar radiation incident on the absorber. In addition, the optimisation framework is extended to the simultaneous selection of coating materials and layer thicknesses, enabling the exploration and identification of alternative multilayer architectures, particularly for high-temperature operation. Finally, the backside LEC is explicitly included in the thermal analysis, allowing the front-side spectral design, substrate emissivity, and backside radiative losses to be jointly considered for the development of high-performance, robust, and scalable solutions for advanced solar thermal absorbers.

2. Theoretical model

2.1 Theory

The thermodynamic performance of a solar selective absorber (SSA) relies mostly on two main radiative parameters: solar absorptance (α_s) and thermal emittance ($\epsilon(T)$). These physical quantities are determined from the reflectivity spectra $\rho(\lambda)$ of the multilayered coating, which were determined using our code based on the transfer matrix approach for thin films (Macleod, 2021).
In fact, since for opaque materials transmissivity is zero ($\tau(\lambda) = 0$), the energy conservation law implies that reflectivity represents the complement of absorptivity, as reported in the following equation:

$$\alpha(\lambda) = 1 - \rho(\lambda) \qquad \text{(eq. 1)}$$

In a standard approach, the solar absorptance is evaluated by integrating the absorptivity, according to (eq.1), weighted by the standard AM1.5 solar irradiation spectrum S(λ)[$\mathrm{W\,m^{-2}\,\mu m^{-1}}$]. However, to properly model the realistic operating conditions of HVFPCs, the conventional solar absorptance evaluation is modified, i.e., the standard solar spectrum $S(\lambda)$ is replaced by an effective incident spectrum, defined as the product of the standard solar irradiance and the wavelength-dependent transmittance of the glass envelope, $\tau_{glass}(\lambda)$. The modified solar absorptance is thus expressed as follows:

$$\alpha_S = \frac{\int_{0.3\,\mu\mathrm{m}}^{2.5\,\mu\mathrm{m}}[1-\rho(\lambda)]S(\lambda)\tau_{glass}(\lambda)d\lambda}{\int_{0.3\,\mu\mathrm{m}}^{2.5\,\mu\mathrm{m}} S(\lambda)\tau_{glass}(\lambda)d\lambda} \quad \text{(eq. 2)}$$

For simplicity, glass transparency is considered spectrally uniform in most cases ($\tau_{glass}(\lambda) = \tau$). According to Kirchhoff's law of thermal radiation, for a given surface at thermodynamic equilibrium, absorptivity and emissivity are equal:

$$\alpha(\lambda) = \epsilon(\lambda) \quad \text{(eq. 3)}$$

So, this means that thermal emittance ($\epsilon(T)$) can be calculated by weighting the absorptivity (eq. 1) with the blackbody radiation spectrum $E_{bb}(\lambda, T)$ [$\mathrm{W\,m^{-2}\,\mu m^{-1}}$] as follows:

$$\epsilon(T) = \frac{\int_0^{\infty}[1-\rho(\lambda)]E_{bb}(\lambda,T)d\lambda}{\int_0^{\infty} E_{bb}(\lambda,T)d\lambda} \quad \text{(eq. 4)}$$

On the basis of α_s and $\epsilon(T)$, the thermal transfer efficiency of the coating, $\eta_{coat}(T_h)$, can be evaluated as follows:

$$\eta_{coat}(T_h) = \alpha_S - \frac{\epsilon(T_h)\sigma_{SB}(T_h^4 - T_{amb}^4)}{H} \quad \text{(eq. 5)}$$

where $T_h[K]$ is the absorber temperature, $T_{amb}[K]$ is the environment temperature, H [$\mathrm{W\,m^{-2}}$] is the total solar incident power and σ_{SB} [$\mathrm{W\,m^{-2}\,K^{-4}}$] is the Stefan-Boltzmann constant.

However, η_{coat} does not fully represent a real flat-plate absorber, as it neglects the radiative losses from the back side of the substrate. To account for the overall system performance, the overall efficiency η_{all} is introduced by modifying (eq. 5):

$$\eta_{all}(T_h) = \alpha_S - \frac{\epsilon(T_h)\sigma_{SB}(T_h^4 - T_{amb}^4)}{H} - \frac{\epsilon_{sub}\sigma_{SB}(T_h^4 - T_{amb}^4)}{H} \quad \text{(eq. 6)}$$

where ϵ_{sub} denotes the equivalent thermal emittance relative to the absorber backside and the vacuum vessel, which is generally considered temperature-independent. This analytical formulation, previously validated in the literature (De Maio et al., 2021), provides a highly reliable approximation of the actual thermal performance of the solar collector in the case of negligible contribution of conductive losses due to residual gas and contact thermal bridges.

2.2 Optimisation procedure: genetic algorithm

The optimisation procedure that has been followed relies on a Genetic Algorithm (GA) code. Overall, a Genetic Algorithm represents a method that mimics the process of natural selection to implement a heuristic search for problem-solving and that is often used to solve constrained and unconstrained optimisation problems. In the present work, the algorithm was configured to calculate $\rho(\lambda)$ for each SSA layer, allowing the determination of the solar absorptance α_s and thermal emittance $\epsilon(T)$, as described in Eqs. (2) and (4), respectively. These two parameters are indeed essential to determine the fitness function of the genetic algorithm, represented by the overall efficiency (Eq. 6). Then, the fitness function was constrained to take into account the structural tolerances to manufacturing errors in layer thickness. Specifically, the genetic algorithm was programmed to set the maximum thermal efficiency loss to 2% even under significant layer thickness variations of 20% (De Maio et al., 2022).

3. Materials and architectures

3.1 The role of glass cover transparency

In real HVFPCs, the solar radiation does not impact directly on the selective solar absorber, but first goes through a glass envelope. Therefore, the spectral distribution of the radiation reaching the absorber is affected by the wavelength-dependent transmittance of the glass cover. Since the solar absorptance depends not only on the intrinsic optical properties of the coating, but also on the spectral distribution of the incident radiation, in this work, the effect of the glass cover transparency on the SSA spectral response has been considered.

Therefore, in the present model, the standard AM1.5 solar spectrum has been modified by introducing the wavelength-dependent glass transmittance, as described in Eq. (2). A glass envelope configuration provided by Guardian Glass, hereafter referred to as Guard-Clarity, and two extra-clear glass envelope configurations from Centrosolar Glas, hereafter referred to as Extra-Clear and Double-Coated, have been considered in the analysis, using their respective spectral transmittance characteristics (Fig. 1).

The three glass configurations exhibit markedly different spectral transmittance behaviours, reflecting the large variety of spectra of commercially available high-performances glasses. While Extra-Clear and Double-Coated glasses show weakly wavelength-dependent transmittance over the investigated spectral range, the Guard-Clarity glass configuration exhibits a pronounced spectral variation, with transmittance decreasing substantially towards the near-infrared region. The influence of the spectral transmittance on the optimisation results is assessed in Section 4.

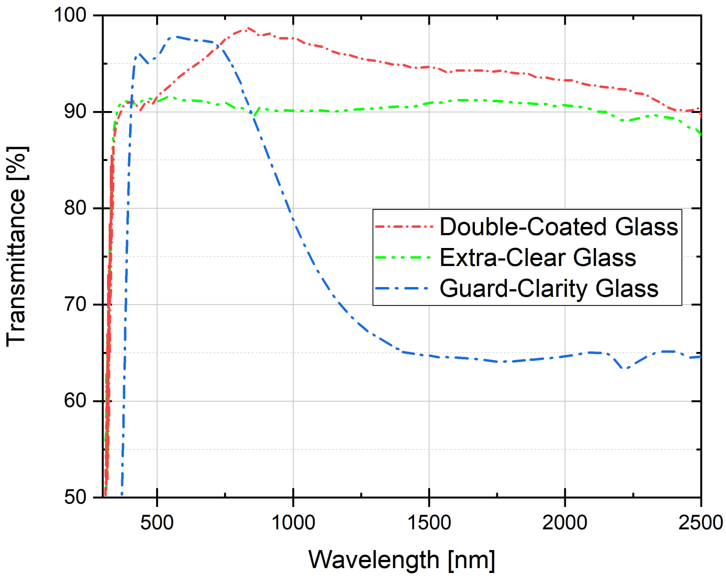

Figure 1: Spectral transmittance curves of the glass envelopes used in the theoretical simulations: two configurations are provided by Centrosolar Glas and one by Guardian Glass. Hereafter, these are referred to as Extra-Clear, Double-Coated, and Guard-Clarity glasses, respectively.

3.2 Multilayer structured coating

A multilayer Selective Solar Absorber (SSA) based on a dielectric-metal-dielectric (DMD) architecture was developed, composed of a Cr_2O_3/Cr multilayer combination (Fig. 2). This architecture represents a traditional optical micro-cavity structure that has shown good optical performance and excellent thermal stability. It is topped with an anti-reflective coating (ARC) based on a SiO_2 layer, whose refractive index lies between those of the external dielectric (air) and chromium oxide. Then, the structure is backed by a low-emissivity copper (Cu) layer (De Maio et al., 2022).

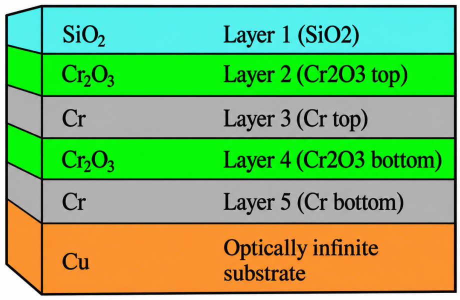

Figure 2: Schematic diagram of multilayer Cr_2O_3/Cr coating.

3.3 Low-Emissivity coating (LEC)

To further reduce radiative losses, it has been considered to decrease thermal emittance not only on the front side of the solar selective absorber, but also on the back side. Building upon previous experimental validations (Caldarelli et al., 2023), this optimisation has been carried out by simulating the presence of a thin silver (Ag) film on the backside of the absorber. Specifically, the LEC was integrated into the numerical framework by directly assigning the silver characteristic emissivity value (ϵ_{sub} = 0.01) to the substrate. This allowed the genetic algorithm to evaluate the overall collector efficiency by optimising, at the same time, the front-side multilayer stack, while accounting for the reduced backside thermal emittance.

4. Results and Discussion

4.1 Impact of the glass spectral transmittance

The selective solar absorbers described in Section 3.2, based on Cr_2O_3/Cr multilayer structures, were designed and optimised for absorber operating temperatures of 100 °C and 300 °C (Table 1). As outlined in the theoretical section, the optimisation framework included the wavelength-dependent transmittance of the glass envelope, aiming for a more realistic design process. To further investigate this effect, the analysis was performed considering the three glass configurations mentioned above in Section 3: Guard-Clarity, Extra-Clear, and Double-Coated glasses. As shown in Figure 1, the three glass configurations exhibit different spectral transmittance behaviours, and this feature is reflected in the optimisation results, reported in Table 1. For Extra-Clear and Double-Coated glasses, the use of an integrated transmittance value leads to almost identical overall efficiencies. Instead, for Guard-Clarity glass, a slightly appreciable difference in overall efficiency is observed, especially at 300 °C. These results carry an important practical implication: the relevance of adopting a wavelength-dependent transmittance increases with the degree of spectral non-uniformity of the glass envelope. While an integrated transmittance provides a suitable approximation for highly transparent and spectrally uniform glasses, such as Extra-Clear and Double-Coated, accounting for the spectral dependence becomes more relevant for configurations such as Guard-Clarity, characterised by a more pronounced variation in transmittance with wavelength.

To further investigate how these differences in glass transmittance affect the spectral response of the optimised absorber, the corresponding spectral absorptance curves are analysed at 300 °C for the three glass configurations (Fig. 3). Despite the different spectral transmittance characteristics of the glass envelopes, the optimised absorbers exhibit a broadly similar spectral response, with high absorptance over the main solar spectral range and a progressive decrease towards longer wavelengths. However, the optimisation leads to slightly different spectral profiles and multilayer thickness combinations depending on the glass configuration (Table 1). This indicates that the wavelength-dependent transmittance of the glass does not simply scale the absorbed solar radiation, but can also influence the spectral characteristics of the optimised absorber. The effect becomes relevant for Guard-Clarity, whose more pronounced spectral variation leads to a larger difference between the wavelength-dependent and integrated-transmittance approaches, as quantified by the overall efficiency values reported in Table 1. This confirms that the spectral characteristics of the glass envelope should be considered during SSA optimisation when there are significant wavelength-dependent variations in transmittance.

Table 1: Optimal thickness combinations, solar absorptance α_s, thermal emittance $\epsilon(T)$, coating efficiency η_{coat} and overall efficiency η_{all} values (ϵ_{sub}:0.02).

Samples	T opt. (°C)	Layer thick. (Layer 1 to 5) (nm)	α_S	$\alpha_S \cdot \tau(\lambda)$	$\epsilon(T)$	η_{coat}	η_{all}
GUARD-CLARITY (τ: 0.876)	100	75-60-9-47-41	0.967	0.848	0.047	0.936	0.804
GUARD-CLARITY	100	78-61-10-48-32	0.964	0.851	0.043	0.936	0.810
GUARD-CLARITY (τ:0.876)	300	58-43-10-19-7	0.886	0.776	0.025	0.744	0.516
GUARD-CLARITY	300	61-40-9-12-9	0.867	0.782	0.023	0.745	0.538
EXTRA-CLEAR (τ: 0.906)	100	76-62-10-46-37	0.966	0.875	0.045	0.936	0.833
EXTRA-CLEAR	100	75-60-10-48-37	0.967	0.876	0.046	0.937	0.833
EXTRA-CLEAR (τ:0.906)	300	63-46-10-14-10	0.888	0.804	0.026	0.740	0.543
EXTRA-CLEAR	300	59-45-10-14-9	0.882	0.800	0.025	0.741	0.543
DOUBLE-COATED (τ: 0.956)	100	78-62-10-48-37	0.967	0.925	0.047	0.936	0.881
DOUBLE-COATED	100	77-64-10-51-37	0.968	0.927	0.048	0.936	0.883
DOUBLE-COATED (τ:0.956)	300	64-41-8-18-11	0.887	0.848	0.026	0.739	0.587
DOUBLE-COATED	300	64-41-11-17-6	0.884	0.849	0.025	0.742	0.590

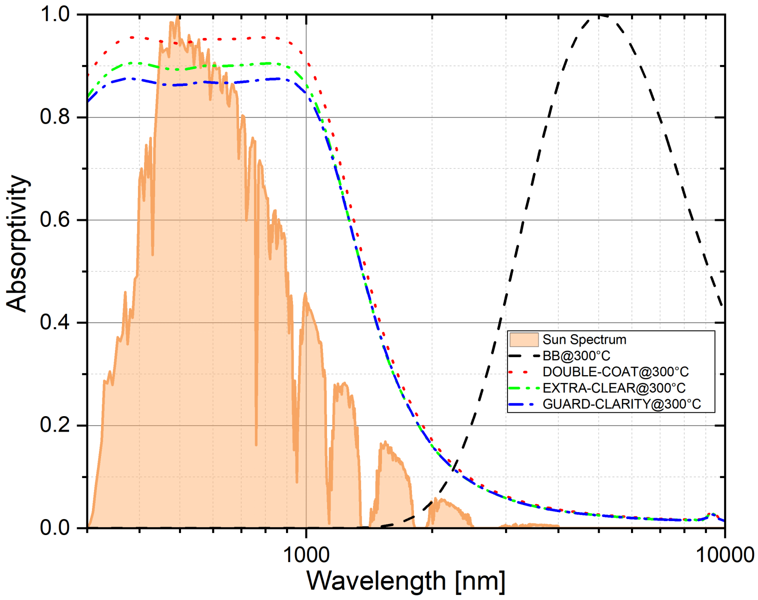

Figure 3: Absorptivity of the optimised SSAs at 300 °C for Double-Coated, Extra-Clear, and Guard-Clarity configurations. The AM1.5 solar spectrum and blackbody (BB) emission curves are also shown in arbitrary units.

4.2 Effect of Low-Emissivity Coating (LEC)

While the adoption of a spectral transmittance-based optical model has shown only a limited impact on the overall performance, the integration of a low-emissivity substrate has instead been a successful strategy for optimising HVFPCs at high operating temperatures. The effect of reducing the absorber backside emissivity on the overall collector efficiency is indeed shown in Fig. 4, for the Extra-Clear and Double-Coated configurations. For both glass configurations, the curves obtained by introducing a LEC (represented by $\epsilon_{\mathrm{sub}} = 0.01$) progressively diverge from those obtained by setting a copper substrate (characterised by $\epsilon_{\mathrm{sub}} = 0.02$), as the operating temperature increases, highlighting the growing importance of backside radiative losses at elevated temperatures. At 100 °C, the reduction in substrate emissivity results in only a limited improvement in collector efficiency. A substantially different behaviour is observed at 300 °C, where the introduction of the low-emissivity backside configuration results in relative collector efficiency improvements of up to approximately 10%, for both the Extra-Clear and Double-Coated configurations. This stronger effect at elevated temperature is consistent with the increasing contribution of backside radiative losses, which scale with the fourth power of the absorber temperature according to Eq. (6), and highlights the importance of low-emissivity backside configurations for high-temperature HVFPC operation.

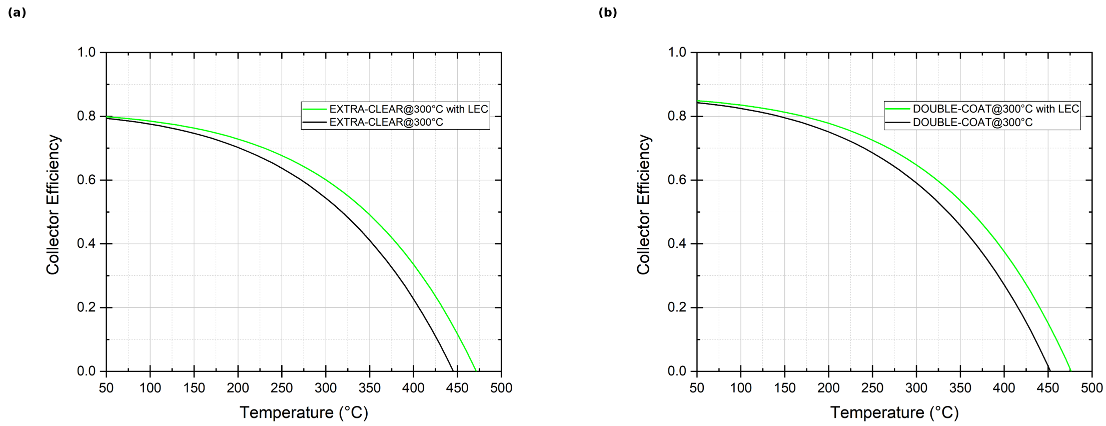

Figure 4: Collector efficiency curves of the optimised coatings at 300 °C, shown with and without LEC as green and black lines, respectively, for (a) Extra-Clear and (b) Double-Coated glass configurations

4.3 Optimisation results: extended material architectures

As the operating temperature increases, the balance between solar absorptance and thermal emittance changes, motivating the search for alternative materials that may provide a more convenient optical and thermal trade-off than the reference Cr_2O_3/Cr architecture.

Accordingly, the optimisation framework has been extended, allowing the genetic algorithm to explore alternative multilayer architectures beyond the $SiO_2/Cr_2O_3/Cr/Cr_2O_3/Cr$ structure. For this analysis, the extended material search was performed for the Extra-Clear and Double-Coated glass configurations, at absorber temperatures of 100 °C and 300 °C. The corresponding optimisation results are reported in Table 2, together with the overall efficiencies of the reference Cr_2O_3/Cr configuration.

At 100 °C, the extended material search does not provide a significant improvement over the reference architecture with the optimised solutions having overall efficiencies comparable to the corresponding reference values. At 300 °C, instead, the enlarged design space enables the identification of alternative multilayer architectures providing higher overall efficiencies. For the copper-substrate configuration ($\epsilon_{\mathrm{sub}} = 0.02$), the relative improvement reaches approximately 8% for Extra-Clear and 6% for Double-Coated. A similar behaviour is obtained when the silver low-emissivity configuration ($\epsilon_{\mathrm{sub}} = 0.01$) is considered, with relative improvements of approximately 7% and 5%, respectively.

Comparing the optimisation results reported in Table 2 with the reference configurations in Table 1, the alternative material designs show a better preservation of the main radiative properties across the two optimisation temperatures. In particular, the decrease in solar absorptance from 100 °C to 300 °C is reduced from approximately 9% to 6% for the Extra-Clear configuration and from approximately 9% to 7% for the Double-Coated configuration. At the same time, the relative reduction in thermal emittance is also less pronounced for the different material simulations. This behaviour suggests that the extended material optimisation allows the solar absorptance to be better preserved at higher operating temperatures, while still achieving low thermal emittance.

Table 2: Optimal thickness combinations, solar absorptance α_s, thermal emittance $\epsilon(T)$, coating efficiency η_{coat}, overall efficiency $\eta_{all}^{\mathrm{opt}}$ values and overall efficiency $\eta_{\mathrm{all}}^{\mathrm{ref}}$ of the reference Cr_2O_3/Cr multilayer structure ($\epsilon_{\mathrm{sub}} = 0.02$).

Samples	T opt. (°C)	Layer thick. (Layer 1 to 5) (nm)	Materials	α_{S}	$\alpha_{\mathrm{S}} \cdot \tau_{\mathrm{glass}}(\lambda)$	$\epsilon(T)$	η_{coat}	$\eta_{\mathrm{all}}^{\mathrm{opt}}$	$\eta_{\mathrm{all}}^{\mathrm{ref}}$
EXTRA-CLEAR	100	75-60-10-48-37	SiO_2-Cr_2O_3-Cr-Cr_2O_3-Cr	0.967	0.876	0.046	0.937	0.833	0.833
DOUBLE-COATED	100	74-52-30-25-34	SiO_2-Cr_2O_3-Cu_2O-Cr-AlN	0.960	0.920	0.035	0.937	0.883	0.883
EXTRA-CLEAR	300	69-29-25-10-2	MgO-SiC-Cr-Cu_2O-a-Si	0.902	0.818	0.020	0.788	0.586	0.543
DOUBLE-COATED	300	34-45-26-10-13	SiO_2-Al_2O_3-SiC-Cr-Cr_2O_3	0.892	0.856	0.021	0.773	0.623	0.590

5. Conclusions

This work presents an integrated optimisation framework for high-vacuum flat plate solar collectors, combining multilayer selective solar absorber design, wavelength-dependent glass transmittance, backside emissivity reduction, and an extended material design space. The Cr_2O_3/Cr-based coatings enable high solar absorptance together with low thermal emittance, providing a suitable reference architecture for medium-temperature operation. The analysis of the glass envelope shows that accounting for its wavelength-dependent spectral transmittance provides a more realistic design criterion than assuming a constant transmittance. While the latter results in only limited variations in the overall collector efficiency for the investigated Extra-Clear and Double-Coated configurations, a more pronounced effect is observed for the Guard-Clarity glass, characterised by stronger spectral variations in transmittance. In contrast, introducing an Ag-based LEC to reduce backside emissivity, substantially improves collector efficiency at 300 °C, with relative gains of about 10% for both glass configurations, highlighting the growing relevance of backside radiative losses at elevated temperatures. Finally, extending the material and thickness design space enables identification of alternative multilayer architectures that provide further improvements in overall efficiency at 300 °C, with a more pronounced relative benefit for the Extra-Clear configuration. Overall, the results show that the performance of HVFPCs at elevated temperature depends on the combined optimisation of the absorber, glass envelope, and backside radiative properties. While the spectral characteristics of the glass become particularly relevant when its transmittance is strongly wavelength-dependent, the reduction of backside emissivity and the extension of the material design space provide additional routes for improving collector efficiency at higher operating temperatures.

Acknowledgements

This work was carried out within a PhD research project funded under the PR Campania FSE+ 2021/2027 programme, Priority 2 – Education and Training, Specific Objective ESO 4.7, Action 2.g.4, within the framework of the "Innovative PhD programmes with industrial characterisation" call (DGR No. 261/2025). The authors gratefully acknowledge the support of the University of Naples Federico II, CNR-ISASI and TRESOL S.r.l. in the framework of the research activities.

References

Burlafinger, K., Vetter, A., and Brabec, C. J. (2015). Maximizing concentrated solar power (csp) plant overall efficiencies by using spectral selective absorbers at optimal operation temperatures. *Solar Energy*, 120:428–

438.

Caldarelli, A., Gaudino, E., De Luca, D., Farooq, U., Musto, M., Di Gennaro, E., and Russo, R. (2023). Low emissivity thin film coating to enhance the thermal conversion efficiency of selective solar absorber in high vacuum flat plate collectors. *Thin Solid Films*, 764:139632.

De Maio, D., D'Alessandro, C., Caldarelli, A., De Luca, D., Di Gennaro, E., Russo, R., and Musto, M. (2021). A selective solar absorber for unconcentrated solar thermal panels. *Energies*, 14:900.

De Maio, D., D'Alessandro, C., Caldarelli, A., Musto, M., and Russo, R. (2022). Solar selective coatings for evacuated flat plate collectors: Optimisation and efficiency robustness analysis. *Solar Energy Materials and Solar Cells*, 242:111749.

Gao, D., Gao, G., Cao, J., Zhong, S., Ren, X., Dabwan, Y. N., Hu, M., Jiao, D., Kwan, T. H., and Pei, G. (2020). Experimental and numerical analysis of an optimized evacuated flat plate solar collector. *Applied Energy*, 269:115129.

IEA (2018). Clean and efficient heat for industry.

IEA (2022). Industrial heat demand by temperature range, 2018.

Macleod, H. (2021). *Thin-Film Optical Filters*. CRC Press, S.l.

Moss, R. W., Shire, G. S. F., Henshall, P., Arya, F., Eames, P. C., and Hyde, T. J. (2018). Performance of evacuated flat plate solar thermal collectors. *Thermal Science and Engineering Progress*, 8:296–306.

Ning, Y., Wang, J., Ou, C., Sun, C., Hao, Z., Xiong, B., Wang, L., Han, Y., Li, H., and Luo, Y. (2020). Nicr–mgf2 spectrally selective solar absorber with ultra-high solar absorptance and low thermal emittance. *Solar Energy Materials and Solar Cells*, 206:110219.

Zhou, Z. H., He, C. Y., and Gao, X. H. (2024). Recent advances of spectrally selective absorbers: Materials, nanostructures, and photothermal power generation. *APL Energy*, 2:011503.